AIAA JOURNAL
Vol. 48, No. 12, December 2010

Acoustic Scattering in the Time Domain Using an Equivalent Source Method

Seongkyu Lee,* Kenneth S. Brentner,† and Philip J. Morris‡
Pennsylvania State University, University Park, Pennsylvania 16802

DOI: 10.2514/1.45132

A numerical method to solve acoustic scattering in the time domain is presented in the present paper. Equivalent sources are embedded within a scattering surface and their strengths are determined as a function of time by the pressure-gradient boundary condition on a scattering surface. Once the strengths are determined, the equivalent sources are used to predict the scattered pressure. Linear shape functions are used to discretize the strength of the equivalent sources in time, and singular value decomposition is used to find the least-squares solution and to overcome potential numerical instabilities. The predictions are found to be in excellent agreement with the exact solutions for sound from a point monopole source and band-passed broadband sound. The method works well even at the irregular frequencies at which internal resonance modes occur. Finally, the method is used to predict the scattering of sound from a moving source. It is shown that the method has the capability to capture aperiodic characteristics very well.

Nomenclature

a	=	radius of a sphere, m
c	=	speed of sound, m s^{-1}
e	=	index of equivalent source
j_n	=	spherical Bessel function of the first kind
k	=	wave number, $k = \omega/c$
l	=	time step index
$\mathbf{M}_e$	=	Mach vector of the e th equivalent source
$M_r\|_e$	=	inner product of the vectors $\mathbf{M}_e$ and $\mathbf{r}_e$
$\dot{M}_r\|_e$	=	inner product of the vectors $\dot{\mathbf{M}}_e$ ($\mathrm{d}\mathbf{M}_e/\mathrm{d}\tau$) and $\mathbf{r}_e$
NE	=	number of equivalent sources
NL	=	number of time indices
$\mathbf{n}$	=	outward unit normal vector to surface
p'_i	=	incident acoustic pressure, Pa
p'_s	=	scattered acoustic pressure, Pa
q_e	=	strength of the e th equivalent source, Pa m^{-2}
$\tilde{q}_e^l$	=	strength of the e th equivalent source at the l th time step, Pa m^{-2}
$\tilde{q}_e^k$	=	strength of the e th equivalent source at the k th time step, Pa m^{-2}
$\dot{q}_e$	=	time derivative of the e th equivalent source strength ($\mathrm{d}q_e/\mathrm{d}\tau$), Pa s^{-1} m^{-2}
$\tilde{\mathbf{q}}^k$	=	vector form of $\tilde{q}_e^k$ where $e = 1, 2, 3, \ldots,$ NE, Pa m^{-2}
R	=	distance between observer and source, m
r	=	distance between observer and the center of a sphere, m
$\mathbf{r}_e$	=	unit radiation vector of the e th equivalent source, m
r_e	=	distance between the surface mesh point and e th equivalent source, $r_e = \|x - y_e\|$, M
r_1	=	the monopole source location, m
ret	=	retarded time
t	=	time, s
$\mathbf{x}_e$	=	position vector of the e th equivalent source, m
$\delta()$	=	Dirac delta function
θ	=	azimuthal angle, deg
τ	=	source time, s
ϕ^l	=	global shape function at the l th time step
ω	=	angular velocity, rad/s

Introduction

ACOUSTIC scattering is an important subject in aeroacoustics. Acoustic waves can be reflected and diffracted by a scattering body in a manner that is frequency and position dependent. For example, a turbofan engine inlet, a helicopter fuselage, a tilt-rotor wing, or a helicopter tail rotor shroud, each may substantially modify the acoustic signal that arrives at a given observer location. Such a modification would change both the magnitude and directivity of the acoustic signal from what would be observed for a free-field noise source. Recently, it was demonstrated that a helicopter fuselage can play a significant role in modifying both the magnitude and directivity of the noise generated by the tail rotor, and that the scattering of tilt-rotor noise can be of significance depending on the relative position of the rotors with respect to the body [1].

Acoustic scattering has been studied mostly in the frequency domain due to the ease of computation, even though this implies periodicity and restricts the solution to a single frequency for each computation. A time-domain approach is better suited for the analysis of more general cases: including broadband noise, which contains many frequencies: and is the only way to investigate nonperiodic or transient events, such as those generated by a moving source or during transient maneuvers. The goal of the present paper is to develop an efficient time-domain numerical method to predict the scattered field, and to demonstrate the benefits of the method for broadband and aperiodic noise.

The boundary element method (BEM) has long been applied to solve acoustic radiation and scattering problems in the frequency domain. The BEM directly calculates the scattered pressure at observer locations without solving in the entire domain. Myers and Hausmann [2] developed a new BEM approach [2] for subsonic moving boundaries using the extended Kirchhoff method for moving boundaries. This extended Kirchhoff formulation was applied to develop a boundary integral solution method for scattering from rigid bodies in uniform rectilinear motion. Gennaretti and Testa [3] developed a boundary integral formulation for sound scattered by elastic moving bodies using the Ffowcs Williams and Hawkings

Presented as Paper 2009-3177 at the 15th AIAA/CEAS Aeroacoustics Conference (30th AIAA Aeroacoustics Conference), Miami, FL, 11–13 May 2009; received 26 April 2009; revision received 1 June 2010; accepted for publication 3 June 2010.

*Postdoctoral Research Associate, Department of Aerospace Engineering; currently Mechanical Engineer, General Electric Global Research Center, 1 Research Circle, Niskayuna, NY 12309; sxl348@psu.edu. Member AIAA.

†Professor, Department of Aerospace Engineering; ksbrentner@psu.edu. Associate Fellow AIAA.

‡Boeing/A. D. Welliver Professor, Department of Aerospace Engineering; pjmaer@engr.psu.edu. Fellow AIAA.

(FW-H) equation. In their paper, the formulation was derived in the time domain but the problems were carried out only in the frequency domain. Other versions of the time-domain BEM for acoustic scattering problems can be found in the literature [4–8]. These references focus on the transient solution for a stationary case. The time-domain BEM consumes considerable computational time compared with the frequency-domain BEM, the solution is found to be very sensitive to the numerical algorithm and time step, and it can be subject to numerical oscillations. These problems have been extensively studied for electromagnetic and elastodynamic BEM problems [9–16]. In addition to these difficulties with the time-domain BEM, the BEM has a well-known numerical issue known as the nonuniqueness problem. It fails to provide a unique solution at certain internal frequencies associated with the resonances of the interior fluid region [17–19]. Mathematically, the matrix becomes ill-conditioned at those frequencies and is not invertible.

Since a time-domain solution could require a considerable increase in computation time compared with the frequency-domain approach and it induces potential numerical issues, an efficient and accurate time-domain method for acoustic scattering problems is desirable. To this end, an approach using a moving equivalent source method is developed in the present paper to predict acoustic scattering in the time domain. The concept of a time-domain equivalent source method was first proposed by Kropp and Svensson [20] and tested for simple radiation and scattering problems. The current paper builds on the idea of their paper, but it implements new numerical schemes including a higher-order time discretization and the description of the motion of the equivalent sources. The method not only maintains the same advantages of the BEM: it is not necessary to obtain a solution in the entire domain; the outer boundary condition is automatically fulfilled; and it does not involve numerical errors associated with wave propagation such as numerical dissipation and dispersion errors: it is also much faster than the BEM since it uses fewer equivalent sources than the surface mesh points and it does not involve surface integrals. In addition, the method does not suffer from the nonuniqueness problem at irregular frequencies. The method can be applied to predict acoustic scattering of the sound generated by an arbitrary moving source by a moving scattering body. In the present paper, the accuracy and efficiency of the new numerical scheme will be assessed by quantitative and detailed validations against exact solutions. Such a detailed study of the accuracy of the time-domain equivalent source method has not been presented previously. Scattering of broadband noise and an aperiodic signal generated by a moving source will be investigated. Owing to its fast and accurate computation, the method is expected to be applied to practical engineering problems.

Time-Domain Moving Equivalent Source Method

In the present work, the total acoustic field is computed as the sum of the incident field from a source and the field scattered by a body. To calculate the incident field, PSU-WOPWOP [21–24], which implements Farassat's formulation 1A [25–27]: an integral representation of FW-H equation [28]: is used. The input data for the noise prediction can be obtained from a wide range of sources, including detailed CFD predictions, less detailed comprehensive analysis, or even experimental data. The scattered field is calculated with the time-domain moving equivalent source method (TDMESM). The computer code is named TIMES (*ti*me-domain *m*oving *e*quivalent *s*ource method). The main idea of the present method is to satisfy the pressure-gradient boundary condition on the scattering surface using equivalent sources located within the surface. The input data required by the time-domain scattering code are the acoustic pressure gradient on the scattering surfaces. This is calculated by PSU-WOPWOP with a recently developed analytical formulation [29]. Figure 1 shows a schematic of the problem-solving procedure. In this section, the mathematical formulation and a numerical algorithm for the TDMESM are presented in detail.

TIMES computes the scattered acoustic field by summing the contributions from each of the equivalent sources located within the scattering body:

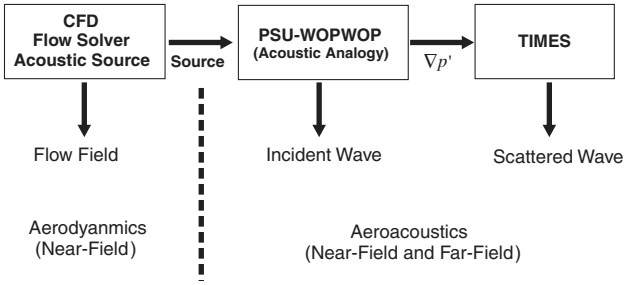

Fig. 1 Schematic of a procedure of predicting the scattered pressure.

$$\Box^2 p'_s = \sum_{e=1}^{\mathrm{NE}} q_e(t)\delta(\mathbf{x}_e) \tag{1}$$

where e is the index of the equivalent source, NE is the number of sources, $q_e(t)$ is the strength of the equivalent sources as a function of time, and $\delta(\mathbf{x}_e)$ is a Dirac delta function acting at the location of the equivalent source, $\mathbf{x}_e$. A smaller replica of the scattering surface is used to locate the equivalent sources inside the scattering body.

To calculate the strengths of the equivalent sources as a function of time, $q_e(t)$, their strengths must be discretized. The strength of an equivalent source is expressed using a global shape function:

$$q_e(t) = \sum_{l=1}^{\mathrm{NL}} \phi^l(t)\tilde{q}_e^l \tag{2}$$

where l is the time index and NL is the number of the time indices. Here $q_e(t)$ is a continuous function with respect to t while $\tilde{q}_e^l$ is defined discretely at each time step l. Note that the strengths, $\tilde{q}_e^l$ are not known a priori, but will eventually be determined. The global shape function, or interpolation function, $\phi^l(t)$ plays the role of interpolating the discrete values of $\tilde{q}_e^l$ onto the function $q_e(t)$. A linear global shape function is used in the current work. It is given by

$$\begin{aligned}
&\phi^l(\tau) = \frac{1}{\Delta\tau}(\tau - \tau^{l-1}) \quad \text{when } (\tau^{l-1} \le \tau \le \tau^l)\\
&\phi^l(\tau) = \frac{1}{\Delta\tau}(\tau^{l+1} - \tau) \quad \text{when } (\tau^{l} \le \tau \le \tau^{l+1})\\
&\phi^l(\tau) = 0 \quad \text{otherwise}
\end{aligned} \tag{3}$$

For rectilinear motion of a body or a stationary body, the boundary condition for an acoustically rigid surface can be written as

$$\frac{\partial p'_s}{\partial n} = -\frac{\partial p'_i}{\partial n} \tag{4}$$

or

$$\nabla p'_s \cdot \mathbf{n} = -\nabla p'_i \cdot \mathbf{n} \tag{5}$$

where p'_i and p'_s are the incident and scattered pressures, respectively, and $\mathbf{n}$ is the outward unit normal vector on the surface. The right-hand side of Eq. (5) is the incident field, which is known. The left-hand side can be determined by using the analytical formulation for the pressure gradient [29] from each of the equivalent sources:

$$4\pi\nabla p'_s = -\sum_{e=1}^{\mathrm{NE}} \left\{ \frac{1}{c}[\hat{\mathbf{r}}_e E_{Te}]_{\mathrm{ret}} + \left[\frac{(\hat{\mathbf{r}}_e - \mathbf{M}_e)q_e}{r_e^2(1 - M_r|_e)^2}\right]_{\mathrm{ret}} \right\} \tag{6}$$

where

$$\begin{aligned}
E_{Te} = &\left[\frac{\dot{q}_e}{r_e(1 - M_r|_e)^2}\right]_{\mathrm{ret}} + \left[\frac{\dot{M}_r|_e q_e}{r_e(1 - M_r|_e)^3}\right]_{\mathrm{ret}}\\
&+ \left[\frac{c(M_r|_e - M_e^2)q_e}{r_e^2(1 - M_r|_e)^3}\right]_{\mathrm{ret}}
\end{aligned} \tag{7}$$

where c denotes the speed of sound, r_e denotes the distance between the surface mesh point and e th equivalent source, $\hat{\mathbf{r}}_e$ denotes the unit

radiation vector, and the subscript ret represents the retarded time, i.e., $\tau = t - r_e/c$ (the time at which the e th equivalent source emits sound to the surface mesh point at time t). Note that the Mach vectors ($\mathbf{M}_e$) are associated with the motion of the e th equivalent source with respect to the ground-fixed frame. $M_r|_e$ denotes the inner product of $\mathbf{M}_e$ and $\hat{\mathbf{r}}_e$, and $\dot{M}_r|_e$ denotes the inner product of $\dot{\mathbf{M}}_e$ and $\hat{\mathbf{r}}_e$. The first term of Eq. (7) includes the time derivative of the source strength ($\dot{q}_e = \mathrm{d}q_e/\mathrm{d}\tau$), the second term depends on the acceleration of the source, and the third term describes the effect of the motion of the source. The sum of the contributions from all the equivalent sources is considered. Equations (6) and (7) to solve Eq. (4) or (5) are new equations developed in the present paper to describe acoustic scattering by a moving body in rectilinear motion or, equivalently, uniform background flow with a stationary body. It is important to note that refraction by nonuniform flow around a body is not included in the current method. To safely neglect the refraction effect, a slender moving body assumption is needed. A complete solution of general scattering problems would need to include the effects of the nonuniform mean flow around the scattering body. Nonuniform mean flow effects could be included through Taylor transformations, which convert the convective wave equation into the wave equation in a stationary flow. This has been achieved in the frequency-domain BEM [30] and ray acoustics [31]. However it should be noted that this is limited to low Mach number potential flows that exclude rotational nonuniform flows, and to high-frequency acoustic disturbances [31]. These conditions are well described in [30]. In the present paper, the Taylor transformation is not implemented and only stationary flows are considered.

For stationary flows, Eq. (4) becomes

$$\frac{1}{4\pi}\sum_{e=1}^{\mathrm{NE}}\left[\frac{1}{cr_{me}}\frac{\partial q_e}{\partial \tau}+\frac{q_e}{r_{me}^2}\right]_{\mathrm{ret}}[\hat{\mathbf{r}}_{me}]_{\mathrm{ret}}\cdot\mathbf{n}=\frac{\partial p'_{i,m}}{\partial n} \tag{8}$$

so the global interpolation function gives

$$\frac{1}{4\pi}\sum_{e=1}^{\mathrm{NE}}\sum_{l=1}^{k}\left[\frac{1}{cr_{me}}\frac{\mathrm{d}\phi^l(\tau_{me})}{\mathrm{d}\tau}\tilde{q}_e^l+\frac{1}{r_{me}^2}\phi^l(\tau_{me})\tilde{q}_e^l\right]_{\mathrm{ret}}[\hat{\mathbf{r}}_{me}]_{\mathrm{ret}}\cdot\mathbf{n}_m = \frac{\partial p'_{i,m}}{\partial n} \tag{9}$$

where subscript me denotes the combination of the surface mesh index m and the equivalent source index e. Equation (9) is evaluated at each surface point (m) and at the current time step, which is denoted by k here.

If the τ_{me} is located between the τ_{me}^- and τ_{me}^+ time steps, where τ_{me}^- is the nearest time step less than the τ_{me} and τ_{me}^+ is the nearest time step larger than the τ_{me}, Eq. (12) can be written using Eq. (3) and its derivative:

$$\frac{1}{4\pi}\sum_{e=1}^{\mathrm{NE}}\left[\left\{\frac{1}{cr_{me}}\left(-\frac{1}{\Delta\tau}\right)\tilde{q}_e^-+\frac{1}{r_{me}^2}\frac{1}{\Delta\tau}(\tau_{me}^+-\tau_{me})\tilde{q}_e^-\right\}+\left\{\frac{1}{cr_{me}}\left(\frac{1}{\Delta\tau}\right)\tilde{q}_e^++\frac{1}{r_{me}^2}\frac{1}{\Delta\tau}(\tau_{me}-\tau_{me}^-)\tilde{q}_e^+\right\}\right]_{\mathrm{ret}}[\hat{\mathbf{r}}_{me}]_{\mathrm{ret}}\cdot\mathbf{n}_m = \frac{\partial p'_{i,m}}{\partial n} \tag{10}$$

where τ_{me}^- and τ_{me}^+ are different for each equivalent source e and surface point m combination. $\tilde{q}_e^-$ and $\tilde{q}_e^+$ represent the strength of the e th equivalent source at the time steps of τ_{me}^- and τ_{me}^+, respectively. Note that Eq. (10) is only true for linear shape functions. If higher-order interpolation functions are used, the equation would be more complicated.

Equation (10) can be rearranged to give

$$\frac{1}{4\pi}\sum_{e=1}^{\mathrm{NE}}\left\{\left[\frac{1}{cr_{me}}\left(\frac{1}{\Delta\tau}\right)+\frac{1}{r_{me}^2}\frac{1}{\Delta\tau}(\tau_{me}-\tau^{k-1})\right]_{\mathrm{ret}}[\hat{\mathbf{r}}_{me}]_{\mathrm{ret}}\cdot\mathbf{n}_m\right\}\tilde{q}_e^k = \frac{\partial p'_{i,m}}{\partial n}+\frac{1}{4\pi}\sum_{e=1}^{\mathrm{NE}}\sum_{l=1}^{k-1}\left[\frac{1}{cr_{me}}\frac{\mathrm{d}\phi^l(\tau_{me})}{\mathrm{d}\tau}\tilde{q}_e^l+\frac{1}{r_{me}^2}\phi^l(\tau_{me})\tilde{q}_e^l\right]_{\mathrm{ret}}\times[\hat{\mathbf{r}}_{me}]_{\mathrm{ret}}\cdot\mathbf{n}_m \tag{11}$$

In Eq. (11) the strength at the current time step, k, is retained on the left-hand side and the strengths at the time steps less than k are moved to the right-hand side because they will have been computed at an earlier time step. It is assumed that strengths for $l < 1$ are zero; thus they are not considered.

A scattering node is influenced by only a few equivalent sources at the current time step. If $\Delta\tau$ is very large, a large number of the equivalent sources can influence the surface point at the current time step so the solution becomes very stable. However, $\Delta\tau$ should be restricted by the highest frequency of interest, because a high-frequency signal requires much smaller $\Delta\tau$ for it to be sufficiently resolved. As a result, as frequency increases, $\Delta\tau$ decreases, and the solution, in turn, becomes more unstable. Also, as the equivalent sources are positioned closer to the surface points, the number of equivalent sources, which contribute to the surface point at the current time step, increases. But placing the equivalent sources closer to the surface could cause numerical errors due to the presence of the $1/r_{me}$ or $1/r_{me}^2$ terms, which become singular as r_{me} goes to zero. A change of the distribution of the equivalent sources could mitigate this problem. An investigation of the choice of the equivalent source distribution will be the subject of future investigation.

Equation (11) can be written in matrix form as follows:

$$\mathbf{A}\,\tilde{\mathbf{q}}^k = \mathbf{B} \tag{12}$$

where $\tilde{\mathbf{q}}^k$ is a vector form of $\tilde{q}_e^k$ where $e = 1, 2, \ldots, \mathrm{NE}$. Again, at the k th time step, the right-hand side of Eq. (12) is formed from the incident field and $\tilde{\mathbf{q}}^l$, where $l = 1, \cdots, k-1$, and the left-hand side is formed from the contribution at the current time step. Before proceeding to the next source time step, the strengths of the equivalent sources are found. This procedure is repeated as the time step k proceeds from 1 to NL. $\mathbf{A}$ and $\mathbf{B}$ can be expressed from Eq. (11) as

$$\mathbf{A}\,(m,e) = \frac{1}{4\pi}\left\{\left[\frac{1}{cr_{me}}\left(\frac{1}{\Delta\tau}\right)+\frac{1}{r_{me}^2}\frac{1}{\Delta\tau}(\tau_{me}-\tau^{k-1})\right]_{\mathrm{ret}}[\hat{\mathbf{r}}_{me}]_{\mathrm{ret}}\cdot\mathbf{n}_m\right\} \tag{13}$$

$$\mathbf{B}\,(m) = \frac{\partial p'_{i,m}}{\partial n}+\frac{1}{4\pi}\sum_{e=1}^{\mathrm{NE}}\sum_{l=1}^{k-1}\left[\frac{1}{cr_{me}}\frac{\mathrm{d}\phi^l(\tau_{me})}{\mathrm{d}\tau}\tilde{q}_e^l+\frac{1}{r_{me}^2}\phi^l(\tau)\tilde{q}_e^l\right]_{\mathrm{ret}}[\hat{\mathbf{r}}_{me}]_{\mathrm{ret}}\cdot\mathbf{n}_m \tag{14}$$

The matrix is usually a rectangular matrix since fewer equivalent sources are used than surface points, where the boundary condition is satisfied. The matrix equation is solved using singular value decomposition (SVD) to find the least-squares solution of the system. The strength at the current time step is obtained using the strength of the equivalent sources determined at the previous time steps. As is commonly the case in a time-domain method, the solution can become unstable, which means the solution may diverge as the time marching proceeds. This occurs when the time step and position of the equivalent sources are not adequately determined or the system is ill-conditioned. An attractive feature of using SVD is that it regularizes the ill-conditioned matrix, by setting very small singular values (below the cutoff singular value) to zero. A parameter, *eps*, is introduced to determine the cutoff singular value

such that eps $= w_c/w_{\max}$ where w_c is the cutoff singular value and $w_{\max}$ is the maximum singular value. In the current paper, *eps* is chosen to be 0.1. A useful side effect of using the SVD procedure is that while it regularizes the matrix, it also reduces its size, thus reducing the size of the computation.

Numerical Results

Validation Case 1: Scattering of Sound by a Sphere

For the validation of the current time-domain approach, scattering of sound from a monopole source by a sphere is considered first. A schematic of the problem is shown in Fig. 2. The center of sphere (radius 1 m) is located at the origin and the source is at (2,0,0) m. θ is measured counterclockwise from the $+x$ axis. The speed of sound is set to be 340 m/s and the ambient density is 1.213 kg/m^3.

Figure 3a shows a contour of the total sound pressure level (SPL) for $ka = 5$ at the observer plane located at $z = 0$; the observer plane is 10.2 m wide with a resolution of 1 m in each direction. A considerable modification of the directivity can be observed due to the presence of the scattering body. (The incident pressure, although not shown here, exhibits simple spherical spreading.) Fig. 3b shows a comparison of the magnitude of the normalized pressure for the prediction and the analytic solution [32] (pressure is normalized such that the amplitude of the incident pressure is equal to 1 at $\theta = 0$ along the azimuthal angle at $r/a = 1.2$). It is found that the prediction is in excellent agreement with the analytic solution for all azimuthal locations. Figure 4 shows the time history of the pressure at $\theta = 180$ deg. The amplitude of the scattered pressure is higher than that of the incident pressure and they are out of phase such that the total pressure amplitude is slightly decreased and the phase is shifted from the original incident wave. The predicted total pressure is compared with the exact solution. Again, the agreement is excellent.

Table 1 shows a comparison of computation time and the maximum error for different combinations of the surface collocation points and equivalent sources. The maximum error is defined as the maximum value of $|p'_{\text{exact}} - p'_{\text{prediction}}|/p'_{\text{ref}} \times 100$ for observers

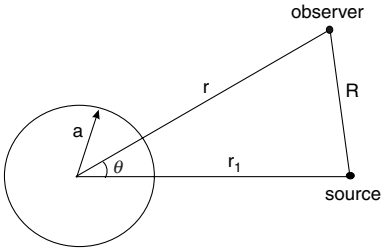

Fig. 2 Schematic of a point source scattering by a sphere.

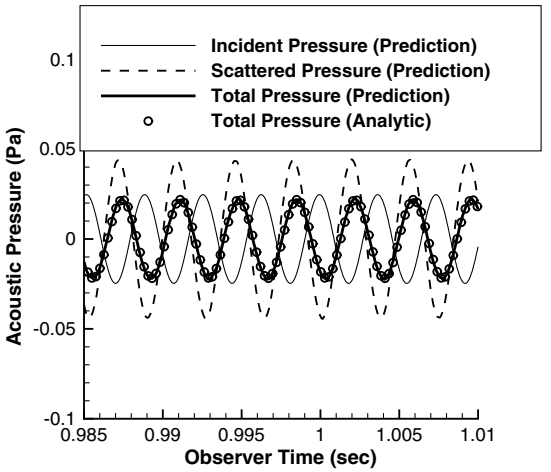

Fig. 4 Comparison of the predicted acoustic pressure with the analytic solution for $ka = 5$ at $r/a = 1.2$ and $\theta = 180$.

along the azimuthal angle at $r/a = 1.2$, where p'_{exact} and $p'_{\text{prediction}}$ are the normalized magnitude for the exact solution and the prediction, and p'_{ref} is chosen to be the source strength instead of p'_{exact} to avoid the division by a value very close to zero around $\theta = 180$ deg. The first three rows in Table 1 use the same ratio of the number of the equivalent sources to the number of the collocation points, i.e., NE $= M/2$ for three different collocation points, where M denotes the number of the collocation points and NE the number of the equivalent sources. The next three rows use the same number of the collocation points ($M = 1024$) and changes the number of the equivalent sources. It can be seen that $M = 1024$ and NE $= 529$ provides a very accurate prediction with an error of 1.8% with computation time of 93 s.

Validation Case 2: Scattering of Sound at the Internal Resonance Frequency

It is well-known that both the frequency-domain and time-domain BEM suffer from a numerical issue known as a nonuniqueness problem. The BEM fails to provide a unique solution at certain internal frequencies associated with the resonances of the interior fluid region (the interior of the scattering body). Mathematically, the matrix becomes ill-conditioned at those frequencies and it is not invertible. A spherical scatterer problem has, for example, irregular frequencies corresponding to ka when $j_n(ka) = 0$ for $n = 0, 1, 2, \ldots$, where j_n denotes the spherical Bessel function of the first kind. The combined Helmholtz integral equation

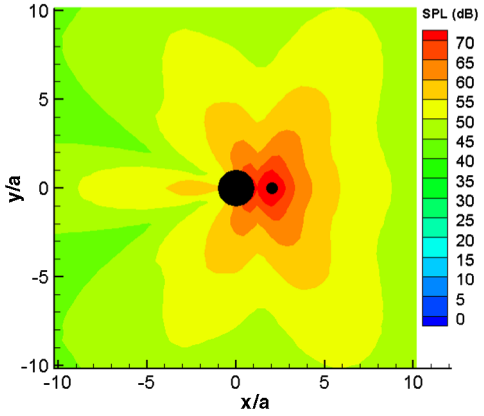

a)

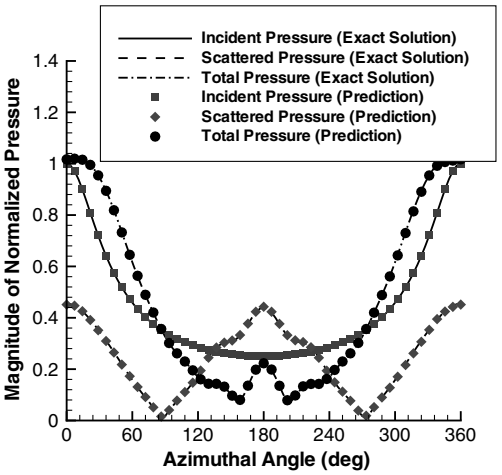

b)

Fig. 3 Directivity of pressure for $ka = 5$: a) SPL of the total pressure at the observer plane and b) comparison between predicted magnitude of the normalized pressures and exact solutions along the azimuthal angle at $r/a = 1.2$.

Table 1 Computation time and the maximum error for the different numbers of the collocation points (M) and the equivalent sources (NE) for $ka = 5$

M	NE	Computation time, s	Error, max., %
2500	M/2	679	0.8
1024	M/2	93	1.8
529	M/2	24	6
1024	529	93	1.8
1024	289	42	4.5
1024	81	16	18

formulation [17], or a method based on second kind of integral equation obtained by differentiating the original boundary integral equation in the normal direction [18], are often implemented in the BEM to overcome this problem. It is interesting and important to investigate the behavior of the predicted results at the irregular frequencies in the TDMESM. For $n = 0$, $ka = \pi$ is a zero of $j_n(ka)$, thus it is selected for the investigation.

Figure 5 shows a comparison of the normalized pressure magnitude as a function of azimuthal angle for observers located at $r/a = 1.2$ from the sphere's center. The prediction is in excellent agreement with the exact solution at all locations. This result demonstrates that the present method works very well even at the irregular frequencies without introducing special treatments.

Validation Case 3: Scattering of Broadband Noise by a Sphere

One of the main advantages of the time-domain method over the frequency-domain method is its capability to predict acoustic scattering of broadband noise efficiently. While the frequency-domain method requires a computation at each frequency, the time-domain method is able to determine the solution at all frequencies in a single computation. Hence the computational saving with the time-domain method can be very large.

A white noise source, that has been filtered to a finite frequency band, is considered as an example case. In this example, the lowest frequency of the band is 54.11 Hz, which corresponds to $ka = 1$, and the highest frequency is 270.56 Hz, which corresponds to $ka = 5$. The frequency step, $\mathrm{d}f$, is set to 0.8 Hz and 4096 points in the time history are used. It can be seen that the entire time signal of the broadband source covers about 67.5 times the period of the lowest frequency and has 12 points per wavelength for the shortest wave. Figure 6 shows the power spectral density of the source as a function of frequency and the time history of the source. The phase at each frequency is set to be zero. The time signal is made by the inverse Fourier transform of the band-passed broadband noise spectrum.

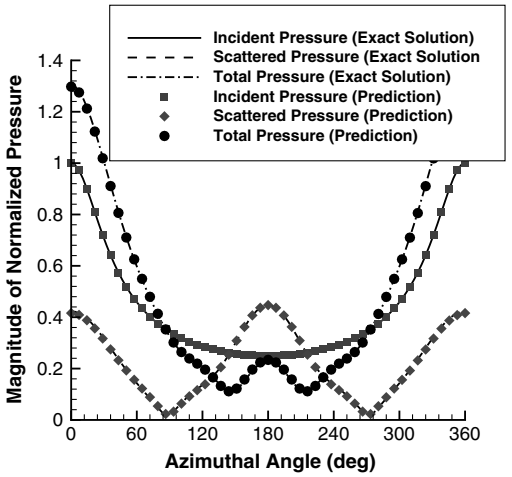

Fig. 5 Comparison of the magnitude of normalized pressure between the prediction and exact solution for $ka = \pi$ as a function of azimuthal angle. The observers are located $r = 1.2$ m from the sphere center.

The change in the predicted acoustic pressure due to scattering by a sphere, is presented at in Fig. 7. Figure 7a shows time history of the incident and total acoustic pressure at $r/a = 1.2$ and $\theta = 154.8$ deg. Although difficult to see in this figure, the amplitude of the acoustic pressure time history is decreased due to the presence of the scattering body at this location. Figure 7b shows SPL as a function of frequency. RMS averaging with 90% overlap was used. It can be seen that SPL decreases with increasing frequency due to diffraction of the sound. The exact solutions for a single frequency of the scattering by a monopole source by a sphere has been computed at several frequencies and are included in the figure. The prediction is in good agreement with the exact solution at each frequency. The very slight discrepancy is thought to be due to the RMS averaging or an imperfect modeling of the band-passed broadband source, and not an error in the prediction of the scattered pressure. A comparison between the prediction and the exact solution was also made at several other observer locations. The prediction was found to be in excellent agreement with the exact solution at all observer positions. Additional validation problems including a two-frequency source (including frequency beating), a dipole source, etc., are given in [33].

Validation Case 4: Scattering of Sound from a Moving Source

Another distinct benefit of the time-domain method is its capability of predicting the scattering of aperiodic sound. Scattering of transient signals has been studied by other methods such as the BEM for the scattering of an electromagnetic field. To the authors' best knowledge, however, the scattering of sound from a moving source has not been solved before. Scattering of sound from a moving source has an important physical characteristic which is different from a simple transient sound. The latter can be decomposed into many frequencies. Therefore, a frequency-domain method could be used to find the solution through the inverse Fourier transform: if not very efficiently. The former, however, manifests itself by the Doppler effect which involves time-varying frequency and amplitude depending on the relative position of the source and the scatterer. This results in a time-dependent and source-motion-dependent pressure field. A time-domain method is the most natural way to predict the scattering of sound from a moving source.

The sound generated from a moving source and scattered by a stationary sphere is considered for $ka = 5$. The monopole source moves from $+y$ to $-y$ with a constant $x/a = 2.0$ position with a Mach number $M = 0.3$. Figure 8 shows the incident, scattered, and total pressure fields at several observer times. As the source moves, the relative position between the source and sphere changes continuously. The scattered and total fields reflect this, in that the pressure contours shown in the plot are curved in a sort of counter-clockwise spiral. This general pattern rotates around the sphere in a clockwise direction (in the plane shown). This complex, time-dependent change in directivity would be difficult, if not impossible, to predict with a frequency-domain method. Furthermore, although in this example the source is moving in rectilinear motion, TIMES could predict scattering with arbitrary source motion as well.

Figure 9 shows the predicted acoustic pressure at four observers ($\theta = 0$, 90, 180, 270 deg relative to the sphere) along $r/a = 1.2$. As can be seen, the amplitude and frequency of not only the incident pressure but also the scattered pressure change over time. The frequency of the incident pressure reproduces the Doppler effect: as the source approaches the observer, the frequency increases, while as the source moves away from the observer, the frequency decreases. It is important that the time-domain approach fully captures this frequency variation. The amplitude of the incident pressure varies not only due to the Doppler effect but also due to the change of the distance between the source and observer. For the scattered pressure, the relative position between the source and observer at any instant time is important to determine the amplitude. For example, for an observer at $\theta = 270$ deg, the scattered pressure decreases as the source approaches the observer, and it increases as the source departs, which is the opposite of the behavior of the incident pressure. This occurs because when the observer is positioned to the side of the scattering body when viewed from the source, the scattered effect is

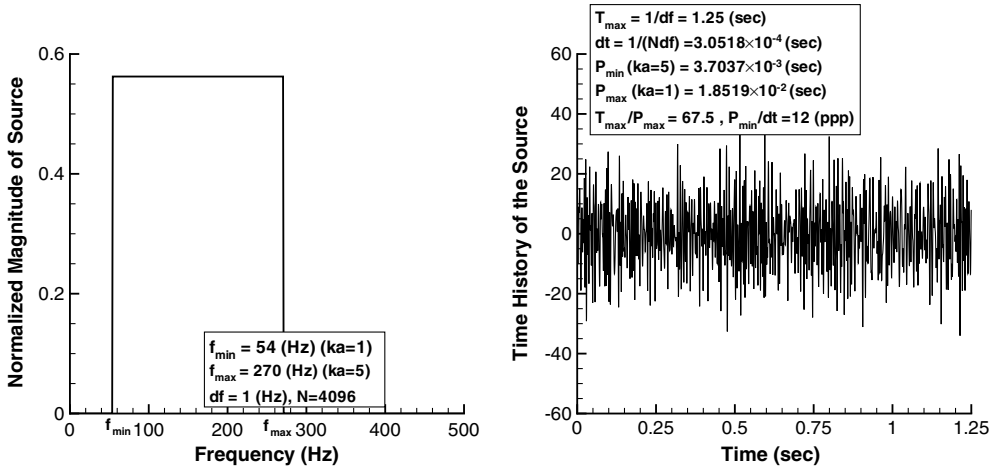

a) b)

Fig. 6 Band-passed broadband noise source with frequencies between 54 Hz or $ka = 1$ and 270 Hz or $ka = 5$: a) mean square in the frequency domain and b) pressure in the time domain.

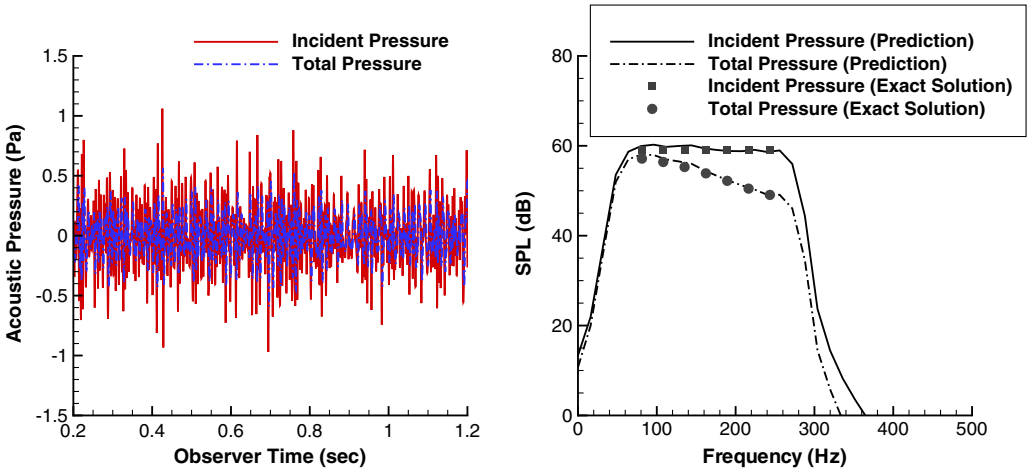

a) b)

Fig. 7 Comparison of the incident and total pressure at $r/a = 1.2$ and $\theta = 154.8$ deg: a) time history of the pressure and b) SPL in the frequency domain.

minimum, and the relative observer position changes over time. The frequency of the scattered pressure is associated with that of the incident pressure, so the frequency of both pressures depends only on the Doppler effect. The total pressure is computed by summing the incident pressure and scattered pressure.

The results for this example have not been fully validated since there is no exact solution or other published data for this case. However, the prediction is qualitatively reasonable based on the observed Doppler effect and the relative position between the moving source, the scatterer, and an observer, and the pressure contour plots and their gradual progression with the motion of the source.

Conclusions

A TDMESM has been developed to efficiently predict acoustic scattering in the time domain. The equivalent sources are embedded within the scattering surface and the strengths of the sources are determined by the boundary condition on the surface. Once determined, the strengths are used to provide the scattered pressure outside the surface. Linear shape functions are used to discretize the source strengths in time and SVD is used to find the least-squares solution and to overcome potential numerical instabilities. The method has been validated against exact solutions and an excellent agreement between the predictions and exact solutions has been achieved for harmonic noise and band-passed broadband noise. In particular, the benefit of the time-domain method is apparent for broadband noise compared with the frequency-domain method since all frequency solutions are obtained at a single computation. In addition, it has been demonstrated that the method works well for an irregular frequency at which internal resonance modes occur. Finally, acoustic scattering of sound from a moving source impinging on a stationary scattering body has been solved. The pressure and pressure gradient are described at each time step and then the method is able to predict the scattering of this aperiodic signal at each time step accordingly. This example clearly illustrates the advantage of the time-domain method over the frequency-domain method for capturing time-dependent frequency and amplitude effects.

This method has been designed originally to solve acoustic scattering of low-frequency problems such as helicopter noise or heavy-lift rotorcraft noise, although there is no limitation to high-frequency problems. When blade thickness noise and stationary loading noise are dominant, only a few harmonics of blade passage frequencies (BPF) are important, and the amplitude of noise drops with increasing frequency. Therefore, the scattering of low-frequency noise by a large dimension of a fuselage can be important for rotorcraft problems. For example, the typical BPF of the main rotor and tail rotor of a full-size BO105 helicopter are around 30 and 70 Hz, respectively. Let us assume a cross-section length of a fuselage to be 1.5 or $a = 0.75$ m. Then, $ka = 5$ yields a frequency of

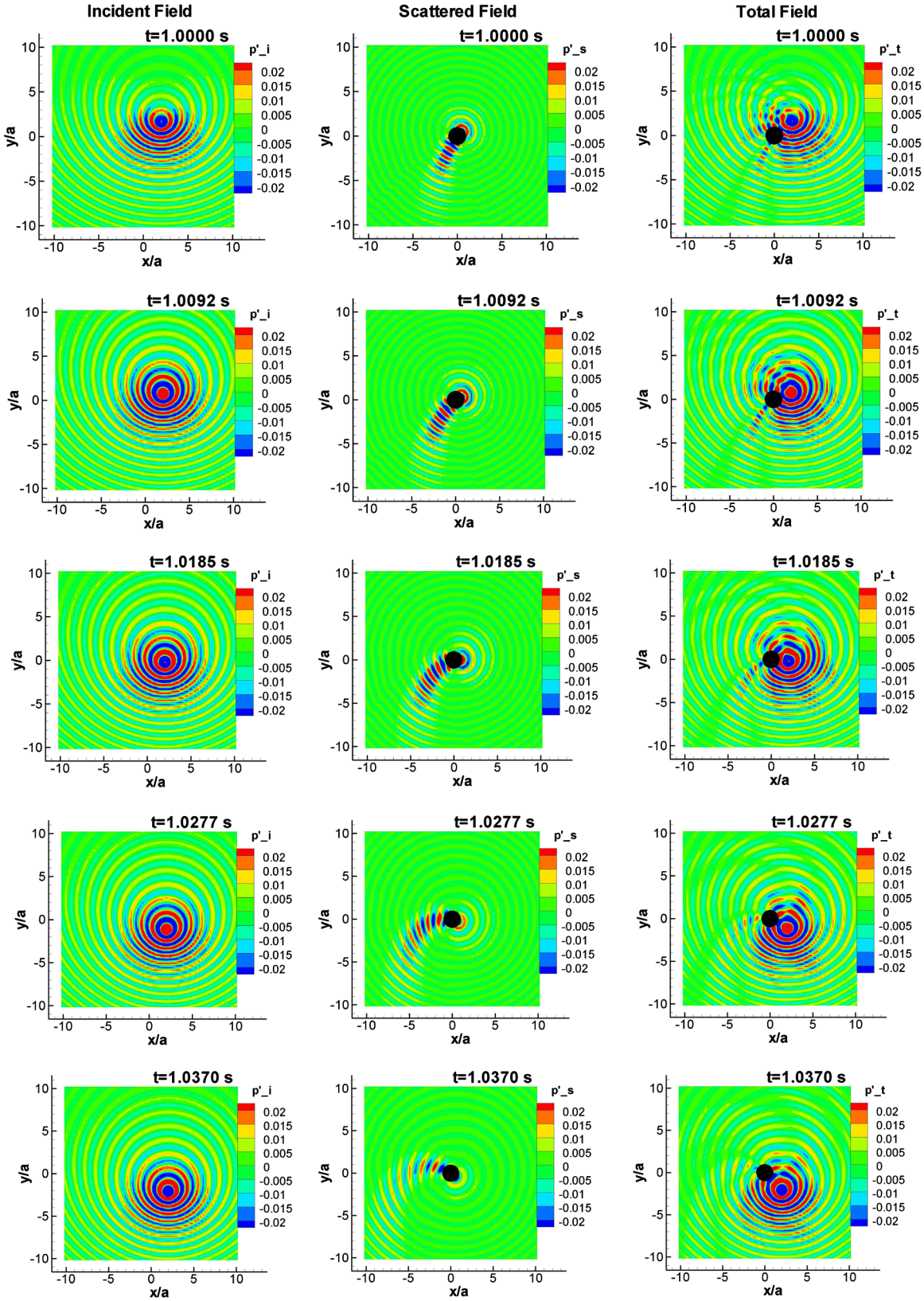

Fig. 8 Contours of acoustic pressure for acoustic scattering by a stationary sphere of a moving source with $ka = 5$ and $M = 0.3$ at several instant times.

360 Hz, which corresponds to the fourth harmonic of the tail rotor BPF or the 11th harmonic of the main rotor BPF. This analysis illustrates that scattering of dominant rotor noise can be predicted when unsteady loading and broadband noise are neglected, in which high frequencies should be resolved. To solve high-frequency problems, the number of collocation points and equivalent sources needs to be increased. Approximately, 10 collocations points per wavelength and half of this number of equivalent sources are needed.

Although the present time-domain scattering method has proved very successful in the prediction of acoustic scattering in the time domain for both broadband noise and noise generated by a moving source, further studies are recommended to continue this research. For example, more complicated geometries such as sharp edges need

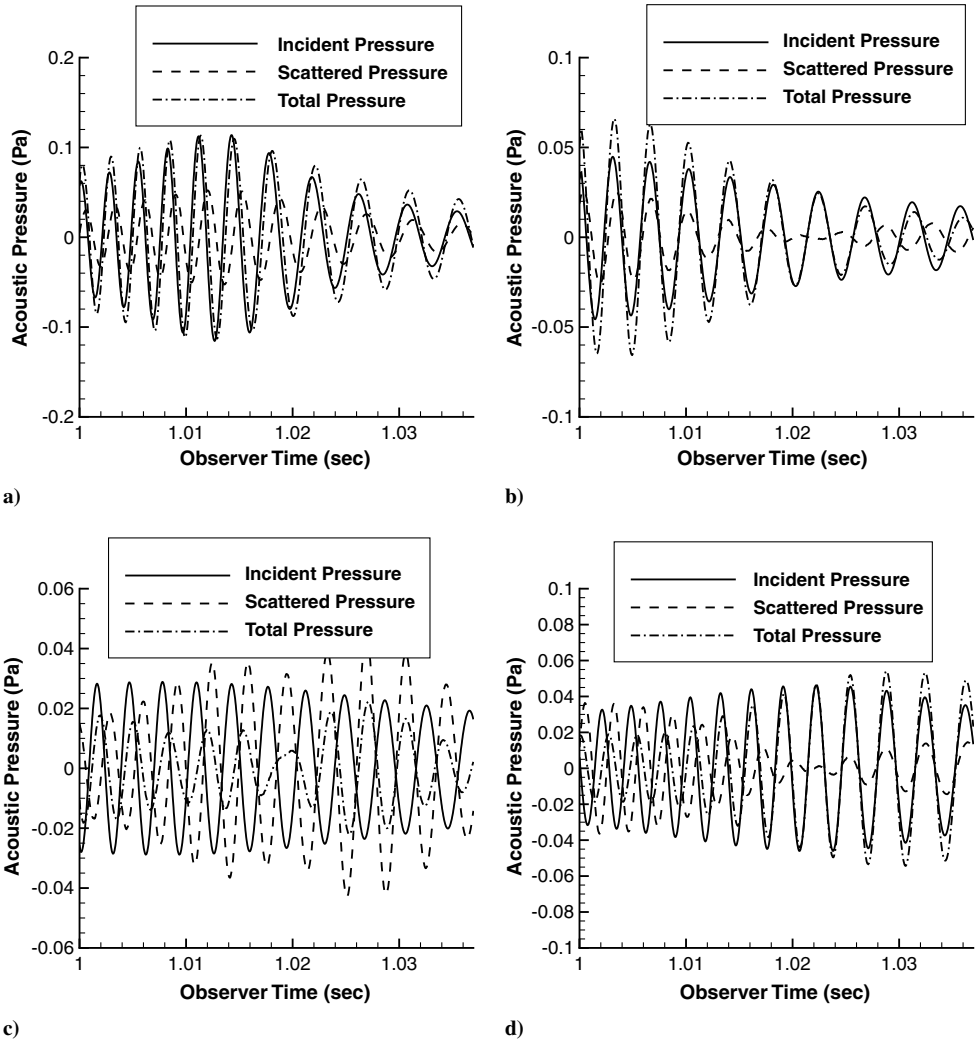

Fig. 9 Predicted acoustic pressure for a moving source with $ka = 5$ and $M = 0.3$ at $r/a = 1.2$ m: a) $\theta = 0$ deg, b) $\theta = 90$ deg, c) $\theta = 180$ deg, and d) $\theta = 270$ deg.

to be considered. A numerical sensitivity study for the parameters used in the method will be investigated. This includes the number and position of the equivalent sources, the time step, and the cutoff singular value implemented in the SVD. A future potential of the current method is the application to the scattering by an arbitrary moving body such as a helicopter in maneuvering flight. This requires a large modification of the boundary condition but can still be managed by using the pressure-gradient formulation for an arbitrary moving body. Finally, a soft boundary condition should be implemented in the future to account for the effect of absorbing materials on a scattering body designed to reduce noise. This requires a time-domain impedance boundary condition.

Acknowledgment

This research was funded by the U.S. Government under Agreement No.W911W6-06-2-0008 under the task of Vertical Lift Research Center of Excellence at Pennsylvania State University.

References

[1] Lee, S., Erwin, J. P., and Brentner, K. S., "A Method to Predict Acoustic Scattering of Rotorcraft Noise," *Journal of the American Helicopter Society*, Vol. 54, No. 4, 2009, p. 042007. doi:10.4050/JAHS.54.042007

[2] Myers, M. K., and Hausmann, J. S., "Computation of Acoustic Scattering from a Moving Rigid Surface," *Journal of the Acoustical Society of America*, Vol. 91, No. 5, May 1992, pp. 2594–2605. doi:10.1121/1.402996

[3] Gennaretti, M., and Testa, C., "A Boundary Integral Formulation for Sound Scattered by Elastic Moving Bodies," *Journal of the Acoustical Society of America*, Vol. 314, Nos. 3–5, 2008, pp. 712–737. doi:10.1121/1.388625

[4] Herman, G. C., and van den Berg, P. M., "A Least-Square Iterative Technique for Solving Time-Domain Scattering Problem," *International Journal for Numerical Methods in Engineering*, Vol. 39, No. 2, 1996, pp. 1419–1431.

[5] Bluck, M. J., and Walker, S. P., "Analysis of Three-Dimensional Transient Acoustic Wave Propagation Using the Boundary Integral Equation Method," *International Journal for Numerical Methods in Engineering*, Vol. 39, No. 8, 1996, pp. 1419–1431. doi:10.1002/(SICI)1097-0207(19960430)39:8<1419::AID-NME911>3.0.CO;2-C

[6] Suchivoraphangpong, V., Walker, S. P., and J., B. M., "Extending Integral Equation Time Domain Acoustic Scattering Analysis to Larger Problems," *International Journal for Numerical Methods in Engineering*, Vol. 46, No. 12, 1999, pp. 1997–2010. doi:10.1002/(SICI)1097-0207(19991230)46:12<1997::AID-NME806>3.0.CO;2-4

[7] Ergin, A. A., Shanker, B., and Michielssen, E., "Analysis of Transient Wave Scattering from Rigid Bodies Using a Burton-Miller Approach," *Journal of the Acoustical Society of America*, Vol. 106, No. 5, 1999, pp. 2396–2404. doi:10.1121/1.428076

[8] Chappell, D. J., Harris, P. J., Henwood, D., and Chakrabarti, R., "A Stable Boundary Element Method for Modeling Transient Acoustic Radiation," *Journal of the Acoustical Society of America*, Vol. 120, No. 1, 2006, pp. 74–80. doi:10.1121/1.2202909

[9] Smith, P. D., "Instabilities in Time Marching Methods for Scattering: Cause and Rectification," *Electromagnetics*, Vol. 10, No. 4, 1990, pp. 439–451. doi:10.1080/02726349008908256

[10] Davies, P. J., and Duncan, D. B., "Averaging Techniques for Time-Marching Schemes for Retarded Potential Integral Equations," *Applied Numerical Mathematics*, Vol. 23, No. 3, 1997, pp. 291–310. doi:10.1016/S0168-9274(96)00069-4

[11] Frangi, A., and Novati, G., "On the Numerical Stability of Time-Domain Elastodynamic Analyses by BEM," *Computer Methods in Applied Mechanics and Engineering*, Vol. 173, Nos. 3–4, 1999, pp. 403–417. doi:10.1016/S0045-7825(98)00294-1

[12] Yu, G., Mansur, W. J., Carrer, J. A. M., and Gong, L., "Stability of Galerkin and Collocation Time Domain Boundary Element Methods as Applied to the Scalar Wave Equation," *Computers and Structures*, Vol. 74, No. 4, 2000, pp. 495–506. doi:10.1016/S0045-7949(99)00025-5

[13] Birgisson, B., Siebrits, E., and Peirce, A. P., "Elastodynamic Direct Boundary Element Methods with Enhanced Numerical Stability Properties," *International Journal for Numerical Methods in Engineering*, Vol. 46, No. 6, 1999, pp. 871–888. doi:10.1002/(SICI)1097-0207(19991030)46:6<871::AID-NME698>3.0.CO;2-6

[14] Walker, S. P., Bluck, M. J., and Chatzis, I., "The Stability of Integral Equation Time-Domain Computations for Three-Dimensional Scattering; Similarities and Differences Between Electrodynamic and Elastodynamic Computations," *International Journal of Numerical Modelling*, Vol. 15, Nos. 5–6, 2002, pp. 459–474. doi:10.1002/jnm.473

[15] Xia, M. Y., Zhang, G. H., and Dai, G. L., "Stable Solution of Time Domain Integral Equation Methods Using Quadratic B-Spline Temporal Basis Functions," *Journal of Computational Mathematics*, Vol. 25, No. 3, 2007, pp. 374–384.

[16] Wang, H., Henwood, D. J., Harris, P. J., and Chakrabarti, R., "Concerning the Cause of Instability in Time-Stepping Boundary Elements Methods Applied to the Exterior Acoustic Problem," *Journal of Sound and Vibration*, Vol. 305, Nos. 1–2, 2007, pp. 289–297. doi:10.1016/j.jsv.2007.03.083

[17] Schenk, H. A., "Improved Integral Formulation for Acoustic Radiation Problems," *Journal of the Acoustical Society of America*, Vol. 44, No. 1, 1968, pp. 41–58. doi:10.1121/1.1911085

[18] Burton, A. J., and Miller, G. F., "The Application Integral Equation Methods to the Numerical Solution of Some Exterior Boundary Value Problems," *Proceedings of the Royal Society of London Series A*, Vol. 323, No. 1553, 1971, pp. 201–210. doi:10.1098/rspa.1971.0097

[19] Amini, S., and Harris, P. J., "A Comparison Between Various Boundary Integral Formulations of the Exterior Acoustic Problem," *Computer Methods in Applied Mechanics and Engineering*, Vol. 84, No. 1, 1990, pp. 59–75. doi:10.1016/0045-7825(90)90089-5

[20] Kropp, W., and Svensson, P. U., "Application of the Time Domain Formulation of the Method of Equivalent Source to Radiation and Scattering Problems," *Acustica*, Vol. 81, No. 6, 1995, pp. 528–543.

[21] Brès, G. A., "Modeling the Noise of Arbitrary Maneuvering Rotorcraft: Analysis and Implementation of the PSU-WOPWOP Noise Prediction Code," M.S. Thesis, Dept. of Aerospace Engineering, Pennsylvania State Univ., University Park, PA, June 2002.

[22] Perez, G., "Investigation of the Influence of Maneuver on Rotorcraft Noise," M.S. Thesis, Dept. of Aerospace Engineering, Pennsylvania State Univ., University Park, PA, June, 2002.

[23] Brès, G. A., Brentner, K. S., Perez, G., and Jones, H. E., "Maneuvering Rotorcraft Noise Prediction," *Journal of Sound and Vibration*, Vol. 275, Nos. 3–5, 2004, pp. 719–738.

[24] Hennes, C., Lopes, L., and Shirey, J., "PSU-WOPWOP User's Manual," Pennsylvania State Univ., University Park, PA, 2005.

[25] Farassat, F., and Succi, G. P., "The Prediction of Helicopter Rotor Discrete Frequency Noise," *Proceedings of the 38th American Helicopter Society Annual Forum*, Anaheim, CA, 4–7 May 1982, pp. 497–507.

[26] Brentner, K. S., "Prediction of Helicopter Discrete Frequency Rotor Noise: A Computer Program Incorporating Realistic Blade Motions and Advanced Acoustic Formulation," NASA TM 87721, 1986.

[27] Farassat, F., "Derivation of Formulations 1 and 1A of Farassat," NASA TM 2007-214853, 2007.

[28] Ffowcs Williams, J. E., and Hawkings, D. L., "Sound Generation by Turbulence and Surfaces in Arbitrary Motion," *Philosophical Transactions of the Royal Society of London. Series A: Mathematical and Physical Sciences*, Vol. A264, No. 1151, 1969, pp. 321–342.

[29] Lee, S., Brentner, K., Farassat, F., and Morris, P., "Analytic Formulation and Numerical Implementation of an Acoustic Pressure Gradient Prediction," *Journal of Sound and Vibration*, Vol. 319, Nos. 3–5, 2009, pp. 1200–1221. doi:10.1016/j.jsv.2008.06.028

[30] Astley, R., and Bain, J., "A Three-Dimensional Boundary Element Scheme for Acoustic Radiation in Low Mach Number Flows," *Journal of Sound and Vibration*, Vol. 109, No. 3, 1986, pp. 445–465. doi:10.1016/S0022-460X(86)80381-9

[31] Agarwal, A., Dowling, A., Shin, H.-C., and Graham, W., "Ray-Tracing Approach to Calculate Acoustic Shielding by a Flying Wing Airframe," *AIAA Journal*, Vol. 45, No. 5, 2007, pp. 1080–1090. doi:10.2514/1.26000

[32] Crighton, D. G., Dowling, A. P., Ffowcs Williams, J. E., Heckl, M., and Leppington, F. G., *Modern Methods in Analytical Acoustics: Lecture Notes*, Springer–Verlag, London, 1992.

[33] Lee, S., "Prediction of Acoustic Scattering in the Time Domain and its Applications to Rotorcraft Noise," Ph.D. Thesis, Dept. of Aerospace Engineering, Pennsylvania State Univ., University Park, PA, Jan. 2009.

J. Astley
Associate Editor